The modelling and prediction of dynamic responses of slender continua deployed in tall structures under long-period seismic excitations

IOP Conf. Series: Journal of Physics: Conf. Series **1048** (2018) 012005 doi:10.1088/1742-6596/1048/1/012005

The modelling and prediction of dynamic responses of slender continua deployed in tall structures under long-period seismic excitations

S Kaczmarczyk

Faculty of Arts, Science and Technology, University of Northampton, St. George's Avenue, Northampton NN2 6JD, UK

stefan.kaczmarczyk@northampton.ac.uk

Abstract. Tall building structures are susceptible to large sway motions when subjected to earthquake excitations. They are particularly affected by long period earthquake ground motions. These low frequency seismic waves resonate with the fundamental mode of the building structure which in turn causes resonance interactions with long slender continua deployed in modular non-structural installations, such as lifts. Damage due to large resonance motions of suspension/ compensating ropes and cables during earthquake are one of the most common modes of failure in high-rise lift installations. In this paper an analytical model to predict the dynamic responses of a suspension rope system installed in a tall host structure under seismic conditions is presented. The model is then used to predict the dynamic performance of the system under earthquake excitations. The predictions can then be used to develop suitable mitigating strategies and protective measures to minimize the earthquake damage.

1. Introduction

Long-period ground motion excitations induced by distant earthquakes can result in resonance and large seismic responses of high-rise buildings in the modern mega cities located in the intra-plate regions such as Hong Kong, Shanghai, New York, Singapore and Dubai [1]. In those conditions severe damage is inflicted to the buildings' structure and/or to their non-structural components such as lifts and escalators [2,3]. In this paper an analytical model to predict the dynamic responses of a cable - mass system which represents a lift suspension rope – car/ counterweight system under seismic conditions is presented. The model is then used to predict the dynamic performance of the system under long-period earthquake excitations.

2. Mathematical model

Figure 1 shows a cable - mass system mounted within a vertical cantilever host structure subject to ground motion $s_0(t)$. The mass M is suspended on the cable of length L and is constrained horizontally within the host structure by a spring – viscous damping element of effective coefficient of stiffness k the coefficient of damping c. The upper end of the cable is passing through O and the height of the structure is $AB = Z_0$. The structure undergoes bending

elastic deformations $\overline{w}(z,t)$ where $0 \le z \le Z_0$, with the displacements at the top end defined as $\overline{w}(Z_0,t) = \overline{w}_0(t)$. The cable - mass - spring system moves vertically within the host structure at transport speed V and acceleration a. The mean quasi-static tension, mass per unit length, modulus of elasticity and cross-sectional area of the cable are denoted as $T^i = \left[M + m(L-x)\right](g-a)$, m, E and A, respectively. The spatial coordinate x is measured from the upper end of the cable downwards as shown. The lateral dynamic displacements of the cable, coupled with the longitudinal displacements $u(x,t)$, are denoted as $v(x,t)$. The lateral and longitudinal motions of mass M are shown as $v_M(t)$ and $u_M(t)$, respectively.

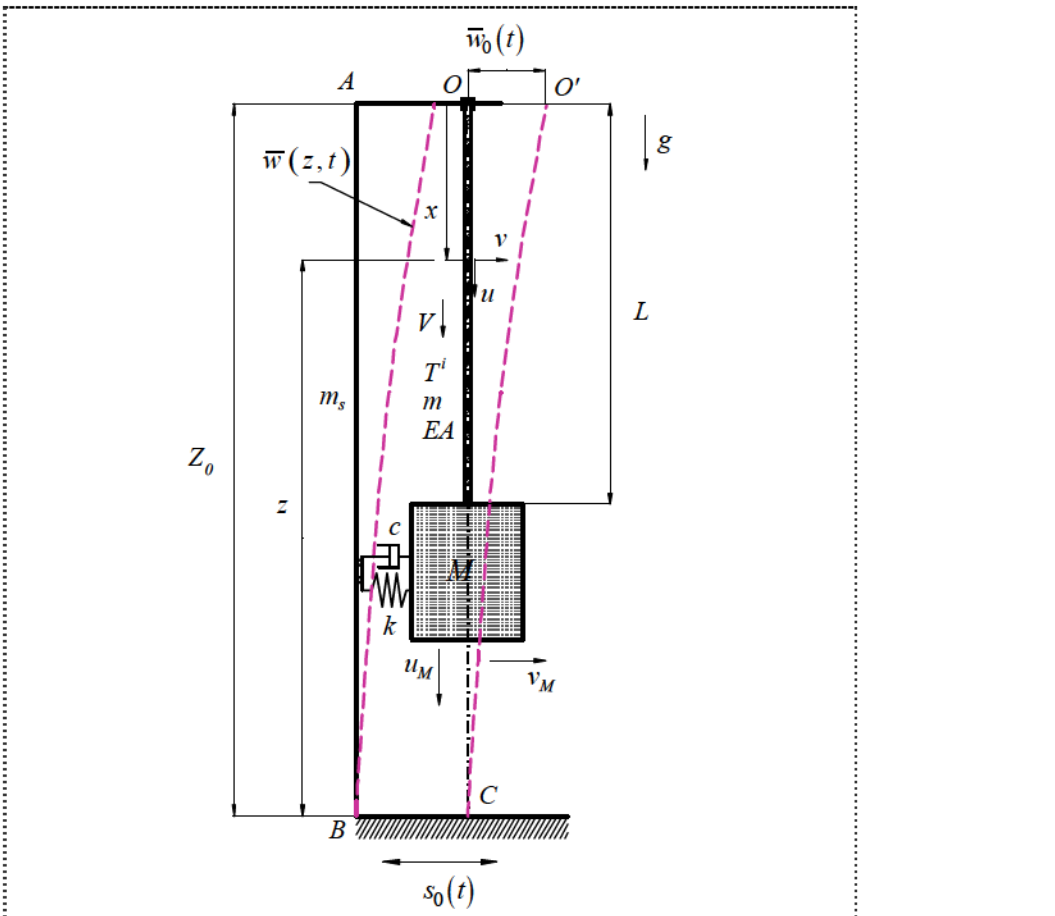

Figure 1. Cable – mass system.

2.1. Model of the structure

The dynamic response of the structure is introduced as the base motion excitation acting upon the cable - mass - spring system. The overall displacements $w(z,t)$ of the structure are described by the following equation

$$m_s(z)w_{tt} + Cw_t + \mathcal{L}w = 0 \tag{1}$$

where $m_s(z)$ the linear mass density of the structure, $\mathcal{L}$ is the spatial operator related to the elastic potential energy of the structure, $\mathcal{C}$ is the damping operator, and $(\ )_t$ denotes the partial derivative with respect to time *t*. The overall displacements of the structure are expressed as

$$w(z,t) = \overline{w}(z,t) + s_0(t) \tag{2}$$

Equation (1) can then be expressed as

$$m_s(z)\overline{w}_{tt} + \mathcal{C}\overline{w}_t + \mathcal{L}\overline{w} = -m_s(z)\ddot{s}_0(t) \tag{3}$$

The solution of (3) can then be assumed in the form of modal expansion

$$\overline{w}(z,t) = \sum_{n=1}^{\infty} W_n(z)p_n(t) \tag{4}$$

where $W_n(z)$ are the eigenfunctions of the structure and $p_n(t)$ are the natural (modal) coordinates. Using equation (4) in equation (3), multiplying the result by W_r integrating over the domain $0<z<Z_0$ and considering the eigenfunction orthogonality conditions the following modal equations are obtained

$$\ddot{p}_r(t) + 2\zeta_r\omega_r\dot{p}_r(t) + \omega_r^2 p_r(t) = P_r(t) \tag{5}$$

where ω_r are the natural frequencies, ζ_r are the modal damping ratios and $P_r(t)$ are the modal excitation terms defined as

$$P_r(t) = -\frac{\ddot{s}_0(t)}{m_r}\int_0^{Z_0} m_s(z)W_r(z)dz \tag{6}$$

where $m_r = \int_0^{Z_0} m_s(z)W_r^2(z)dz$ represents the modal mass. The steady-state response of the structure can then be determined from equation (5) as

$$p_r(t) = \frac{1}{\omega_{dr}}\int_0^t P_r(t-\tau)e^{-\zeta_r\omega_r\tau}\sin\omega_{dr}\tau d\tau \tag{7}$$

where $\omega_{dr} = \omega_r\sqrt{1-\zeta^2}$. If the eigenvalue problem associated with equation (3) does not admit a closed-form solution a set of comparison functions can be used to seek an approximate solution of equation (3) in the following form [4]

$$\overline{w}(z,t) = \sum_{n=1}^{N} \Psi_n(z)q_n(t) \tag{8}$$

where $q_n(t)$ are generalised coordinates. Using equation (8) in equation (3) leads to the following matrix equation of motion

$$\boldsymbol{M}\ddot{\boldsymbol{q}} + \boldsymbol{C}\dot{\boldsymbol{q}} + \boldsymbol{K}\boldsymbol{q} = \boldsymbol{F}(t) \tag{9}$$

where $\boldsymbol{M}=[m_{rn}]$, $m_{rn}=\int_0^{Z_0} m_s\Psi_r\Psi_n dz$, $\boldsymbol{C}=[c_{rn}]$, $c_{rn}=\int_0^{Z_0}\Psi_r C\Psi_n dz$ $\boldsymbol{K}=[k_{rn}]$, $k_{rn}=\int_0^{Z_0}\Psi_r \mathcal{L}\Psi_n dz$, $r,n=1,\ldots N,$ and $\boldsymbol{F}(t)=\left[F_r(t)\right]$, $F_r(t)=-\ddot{s}_0(t)\int_0^{Z_0} m_s\Psi_r dz$ is a vector of generalized excitation forces.

2.2. Governing equations of the cable - mass system

Consider the motions of the cable - mass system. The equations governing the dynamic response of the system are developed by the application of the Hamilton's principle which requires that

$$\int_{t_1}^{t_2}\left(\delta E-\delta\Pi-\delta W_{nc}\right)dt=0,\quad \delta w(x,t)=0 \text{ at } t=t_1,t_2 \tag{10}$$

where E, Π and W_{nc} denote the kinetic energy, the potential energy and the work due to non-conservative forces acting upon the system, respectively. The kinetic energy is given as

$$E=\int_0^L \hat{E}_m(\dot{u},\dot{v})dx+E_M(\dot{u}_M,\dot{v}_M) \tag{11}$$

where

$$\hat{E}_m=\frac{1}{2}m\left[(\dot{u}+V)^2+\dot{v}_M\right] \tag{12}$$

is the kinetic energy density of the cable, and

$$E_M=\frac{1}{2}M\left[(\dot{u}_M+V)^2+\dot{v}_M^2\right] \tag{13}$$

is the kinetic energy of the end mass. Here $u_M=u(L,t)$, $v_M=v(L,t)$, overdots denote the total derivatives with respect to time expressed as $\dot{u}\equiv\frac{Du}{Dt}=u_t+Vu_x$ and $\dot{v}\equiv\frac{Dv}{Dt}=v_t+Vv_x$, with $(\ )_x$ denoting partial derivatives with respect to x, respectively. The potential energy is given as

$$\Pi=\int_0^L\left[\hat{\Pi}_e(u_x,v_x)-mgu\right]dx-Mgu_M+\frac{1}{2}k\Delta^2 \tag{14}$$

where it is k is assumed to be constant and represents the flexibility of the mass guiding system (in the context of a lift system this would be the flexibility of the car roller guide system, the guide rail – guide rail/ bracket system can be considered as rigid). Furthermore the elastic potential energy density of the cable $\hat{\Pi}_e$ is expressed in terms of the Green's strain measure ε as

$$\hat{\Pi}_e=\left(T^i+\frac{1}{2}AE\varepsilon\right)\varepsilon \tag{15}$$

where the Green's strain measure is defined as [5]

$$\varepsilon=u_x+\frac{1}{2}v_x^2 \tag{16}$$

The last term in equation (14) represents the potential energy of the spring deformed by $\Delta=v_M-w_M$ where $w_M=w(Z_0-L,t)$. The work done by the non-conservative damping force is expressed as

$\delta W_{nc} = -c\dot{\Delta}\delta v_M$ so that Hamilton's principle yields the following partial differential equations of motion

$$\begin{aligned} &m\frac{D^2u}{Dt^2} - EA\varepsilon_x = 0, \\ &m\frac{D^2v}{Dt^2} - Tv_{xx} + m(g-a)(xv_{xx} + v_x) - EA(\varepsilon v_x)_x = 0; \\ &M\ddot{v}_M + T^i(L)v_x\big|_{x=L} + c\dot{\Delta} + k\Delta + EA\varepsilon\big|_{x=L} v_x\big|_{x=L} = 0; \\ &M\ddot{u}_M + EA\varepsilon\big|_{x=L} = 0 \end{aligned} \tag{17}$$

where $T = (M + mL)(g - a)$. For tensioned members such as metallic cables the lateral frequencies are much lower than the longitudinal frequencies. Thus, considering that in the case of long-period ground motions the excitations frequencies are much lower than the fundamental longitudinal frequencies the longitudinal inertia of the cable can be neglected in the first equation in (17) [5]. After integrating this equation and using the boundary conditions $u(0,t) = 0$, $u(L,t) = u_M$, the following expression for the quasi-static axial strain in the cable results

$$\varepsilon = u_x + \frac{1}{2}v_x^2 = \frac{u_M}{L} + \frac{1}{2L}\int_0^L v_x^2 dx \equiv e(t) \tag{18}$$

In that way the dynamic model (17) of the system is reduced to three equations of motion.

2.3. Base excitation

In order to develop the model further the assumption is made that the influence of the cable system dynamics on the structural response can be neglected. By considering the scenario in which the structure is subject to fundamental resonance an approximate solution of equation (3) can be sought by using a single-term expansion with the polynomial shape function $\Psi(\eta) = 3\eta^2 - 2\eta^3$ where $\eta = z/Z_0$, applied in equation (8). The base motion excitation is then introduced by expressing the overall lateral displacements of the cable – mass as

$$v(x,t) = \overline{v}(x,t) + s_0(t) + \left(1 + \frac{\Psi_L - 1}{L(\tau)}x\right)\overline{w}_0(t) \tag{19}$$

where $\Psi_L = \Psi\left(\frac{Z_0 - L(\tau)}{Z_0}\right)$ and $\overline{w}_0(t) = \overline{w}(Z_0, t)$. In this formultion L is considered a slowly varying function in time meaning that the change of lenght L over a period corresponding to the fundamental frequency of the system is small compared to the instantaneous value of L [6]. In order to represent this fact a slow time scale defined as $\tau = \epsilon t$, where $\epsilon \ll 1$ is a small parameter, has been introduced. The first term in equation (19) is then expressed

$$\overline{v}(x,t) = \sum_{n=1}^{N} \Phi_n\left[x; L(\tau)\right] q_n(t) \tag{20}$$

where Φ_n are orthogonal trial functions given as

$$\Phi_n\left[x; L(\tau)\right] = \sin\left[\sigma_n(L(\tau))x\right], \quad n = 1,2,\ldots,N \tag{21}$$

The trial functions (21) are defined in terms of the slowly varying eigenvalues σ_n determined by the frequency equation

$$\left(k-\frac{M}{m}T_M\sigma_n^2\right)\sin(\sigma_n L)+T_M\sigma_n\cos(\sigma_n L)=0,\ T_M=T^i(L) \tag{22}$$

By using equation (19) in the reduced system of three equations obtained from (17), and applying the expansion (20) the following set of ordinary differential equations results

$$\ddot{q}_r+2\tilde{\zeta}_r\tilde{\omega}_r\dot{q}_r+\sum_{n=1}^{N}C_{rn}q_n+\tilde{\omega}_r^2q_r+\sum_{n=1}^{N}\left[K_{rn}+\frac{EA}{\tilde{m}_r}\left(\frac{\Psi_L-1}{L}\overline{w}_0\right)^2\left(\frac{1}{L}A_{rn}-\frac{1}{2}\Gamma_{rn}\right)\right]q_n+\frac{EA}{\tilde{m}_rL}\frac{\Psi_L-1}{L}\alpha_r\overline{w}_0u_M$$
$$=\frac{EA}{\tilde{m}_rL}\left[\sum_{n=1}^{N}\Gamma_{rn}q_nu_M+\frac{1}{2}\frac{\Psi_L-1}{L}\overline{w}_0\sum_{i=1}^{N}\sum_{j=1}^{N}\left(2\alpha_i\Gamma_{rj}-\alpha_r\kappa_{ij}\right)q_iq_j+\frac{1}{2}\sum_{i=1}^{N}\sum_{j=1}^{N}\sum_{k=1}^{N}\Gamma_{rk}q_iq_jq_k\right]+\tilde{Q}_r(t;\tau) \tag{23}$$
$$\ddot{u}_M+2\zeta_M\omega_M\dot{u}_M+\omega_M^2u_M+\frac{EA}{ML}\frac{\Psi_L-1}{L}\overline{w}_0\sum_{n=1}^{N}\alpha_nq_n=-\frac{1}{2}\frac{EA}{ML}\sum_{i=1}^{N}\sum_{j=1}^{N}\kappa_{ij}q_iq_j+\tilde{Q}_u(t;\tau)$$

where $\tilde{\zeta}_r$ and ζ_M reperesent the damping ratios and

$$\tilde{\omega}_r^2=\sigma_r^2\frac{T_M}{m};\ \alpha_r=\Phi_r(L),\ \tilde{m}_r=\int_0^L\Phi_r^2dx+M\alpha_r^2,\ A_{rn}=\alpha_r\alpha_n$$
$$K_{rn}=\frac{m}{\tilde{m}_r}\left[g\Psi_{rn}+\left[V^2-L(g-a)\right]\Upsilon_{rn}+(g-a)\Theta_{rn}\right],\ C_{rn}=2\frac{m}{\tilde{m}_r}V\Psi_{rn}+\frac{1}{\tilde{m}_r}cA_{rn}$$
$$\Theta_{rn}=\int_0^L x\Phi_n''\Phi_rdx,\ \Psi_{rn}=\int_0^L\Phi_n'\Phi_rdx,\ \Upsilon_{rn}=\int_0^L\Phi_n''\Phi_rdx,\ \kappa_{ij}=\int_0^L\Phi_i'\Phi_j'dx,\ \Gamma_{rn}=\Upsilon_{rn}-\alpha_r\Phi_n'(L)$$
$$\tilde{Q}_r(t;\tau)=\frac{1}{\tilde{m}_r}\left[Q_r(t;\tau)-\frac{EA}{2}\alpha_r\left(\frac{\Psi_L-1}{L}\overline{w}_0(t)\right)^3\right]; \tag{24}$$
$$Q_r(t;\tau)=-(mX_r+M\alpha_r)\ddot{s}_0-\left[m\left(X_r+\frac{\Psi_L-1}{L}\Pi_r\right)+M\Psi_L\alpha_r\right]\ddot{\overline{w}}_0-2mV\frac{\Psi_L-1}{L}X_r\dot{\overline{w}}_0+$$
$$-\frac{\Psi_L-1}{L}(mgX_r+T_M\alpha_r)\overline{w}_0;\ X_r=\int_0^L\Phi_rdx,\ \Pi_r=\int_0^Lx\Phi_rdx$$
$$\tilde{Q}_u(t;\tau)=-\frac{EA}{2M}\left(\frac{\Psi_L-1}{L}\overline{w}_0\right)^2$$

3. Numerical example and results

A parametric study has been conducted for a model of the cable - mass system comprising the mass M = 3600 kg suspended on 6 steel wire ropes. The ropes have mass per unit length 0.872 kg/m and longitudinal stiffness EA = 22.889 MN, each. Figure 2 shows the variation of the first four lateral natural frequencies of the system when the length of the ropes changes from L_{min} = 58.66 m to L_{max} = 258.66 m. The red solid lines represent the frequencies when the spring constant is k = 66.698 kN/m. The black dashed lines represent the natural frequencies corresponding to the spring of coefficient of elasticity of one order of magnitude higher (k = 666.98 kN/m). In the system with the softer spring the curve veering phenomena can be observed when two eigenvalues approach each other closely and suddenly veer away [7]. For example, the veering regions of the 2nd and the 3rd natural frequency loci and the 3rd and the 4th natural frequency loci correspond to the lengths L of about 125 m and about 193 m, respectively. It is also interesting to observe that the flat sections of the 2nd, 3rd and 4th natural frequency curves correspond to the modes of the mass M motion. The frequency value can be estimated as $\overline{\omega}_M=\sqrt{k/M}=4.3043$ rad/s ($\overline{f}_M=\overline{\omega}_M/2\pi=0.6851$ Hz, shown as the green horizontal

dashed line in figure 2). The first/ fundamental longitudinal natural frequency, corresponding to the frequency $\omega_M = EA/ML$ is also shown in figure 1 (solid blue line).

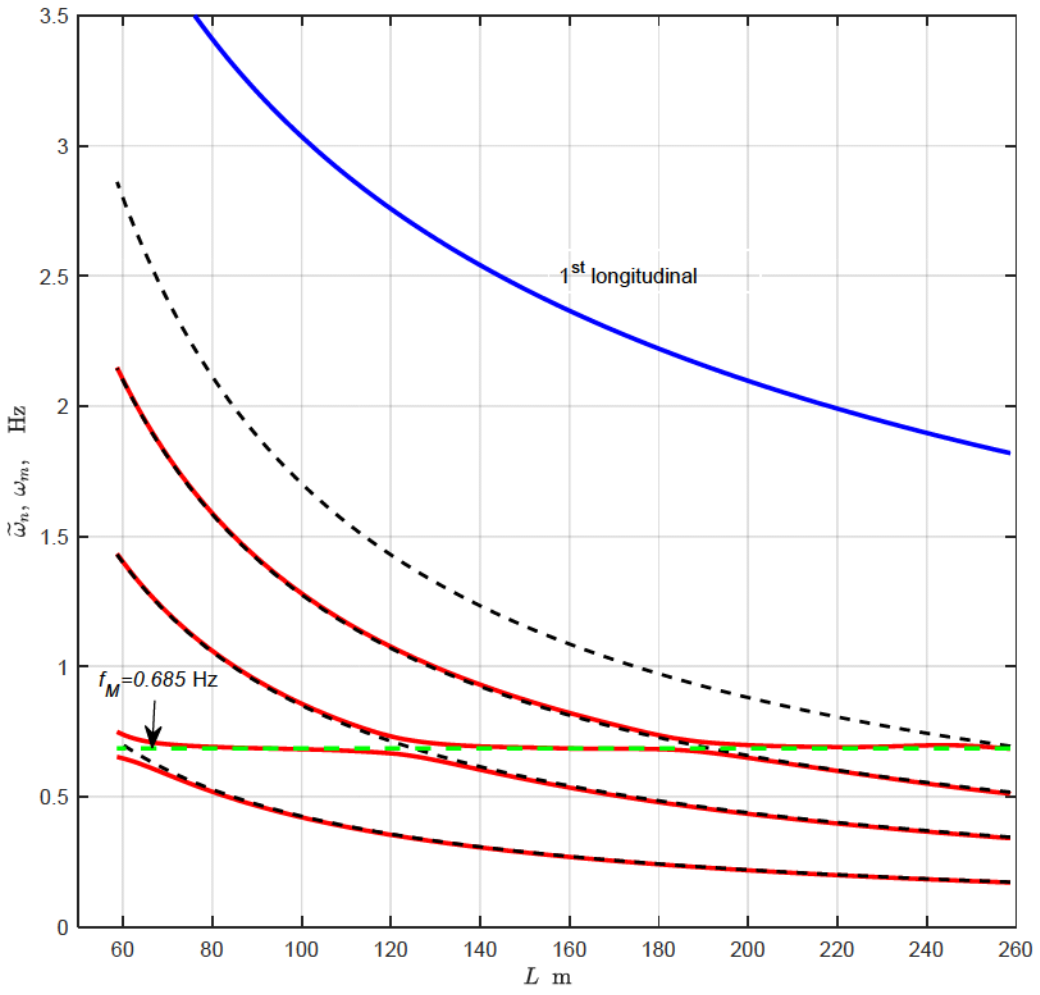

Figure 2. The natural lateral frequencies of the cable - mass system (red solid for k = 66.698 kN/m; black dashed lines for k = 666.98 kN/m), the frequency of the mass M ($\overline{\omega}_M = \sqrt{k/M}$ green solid line) and the 1st longitudinal frequency (blue solid line).

Figure 3 shows the lateral displacements $\overline{v}(x,t)$ of the cable – mass system when the mass is ascending slowly from the lower level upwards at the reduced speed of 0.75 m/s and the length of the ropes changes from about 140 m to 80 m, respectively. The dominant frequency of the ground motion is assumed to be 0.68 Hz (and near $f_M = 0.6851$ Hz), $s_0(t)$ is harmonic with the acceleration magnitude of 0.1 m/s^2. The response of the structure results then in the amplitude of 0.15 m at the top level (corresponding to Z_0). The equations of motion are solved by using six modes in the expansion (20). The 4th-5th order Runge-Kutta algorithm numerical is used to solve the equations of motion numerically assuming the damping ratios $\zeta_1 = 0.003$ for the cable lateral mode, and $\zeta_2 = 0.3$ for the mass lateral mode and $\zeta_M = 0.3$ longitudinal mode, respectively. The response plots in figure 4 and

figure 5 show the lateral displacements $\overline{v}_M$ of the mass, and the longitudinal motions u_M (coupled with the lateral motions) vs. time, respectively. The plots demonstrate resonance behavior of the system. The frequency spectra of the lateral response and the longitudinal response of the mass are shown in figure 6 and figure 7, respectively. The dominant frequency of the longitudinal response is twice the frequency of the excitation (tuned to the lateral resonance frequency of the mass). Thus, the adverse scenario could potentially arise when the longitudinal frequency of the mass near twice the lateral natural frequency of the mass. The longitudinal motions of the mass could then execute the lateral mode of the cable – mass system through the autoparametric coupling.

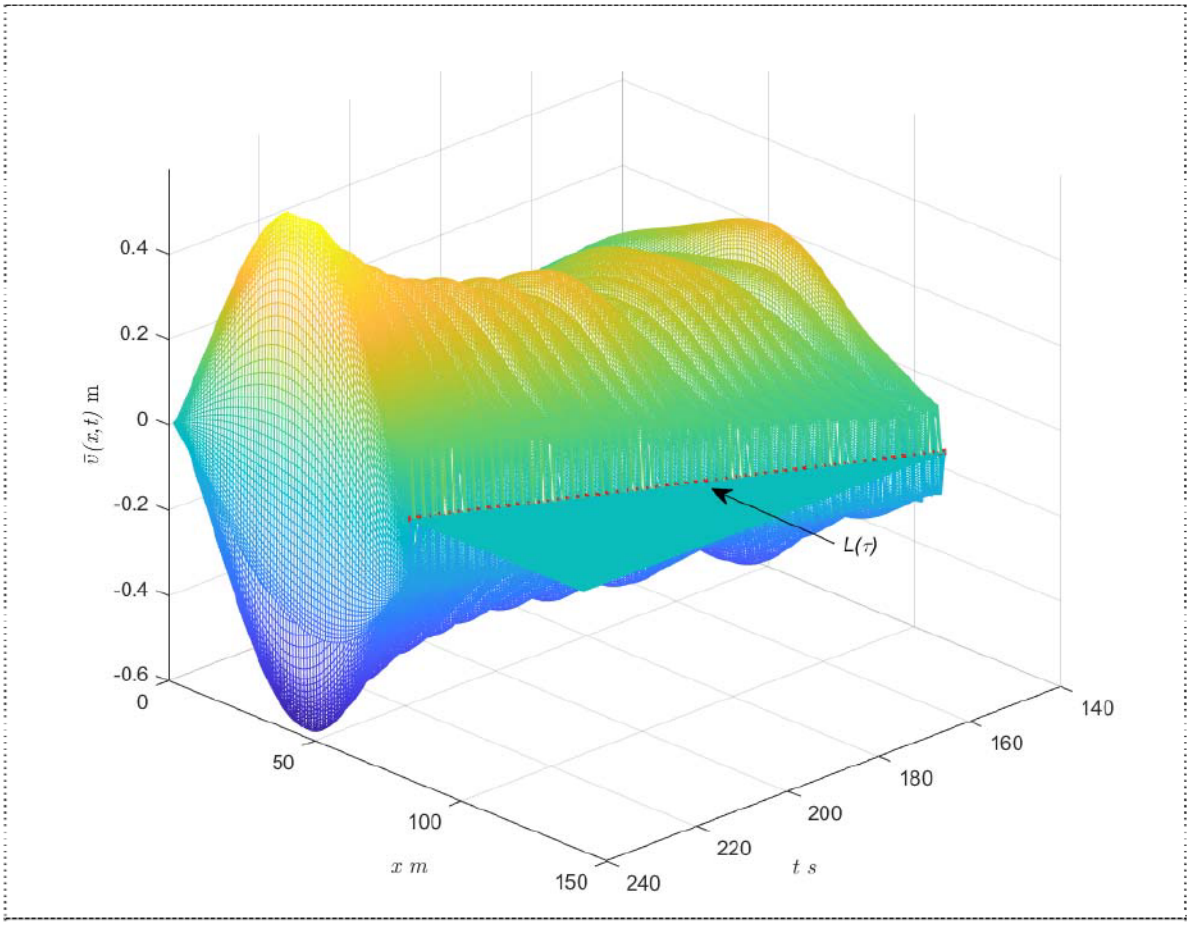

Figure 3. The lateral response $\overline{v}(x,t)$ of the cable - mass system.

4. Conclusions

The dynamic behaviour of a vertical cable – mass system moving slowly within a tall host structure subject to long period seismic excitation is considered in this paper. The proposed mathematical model accommodates the nonlinear effects of cable stretching and is used to determine the response of the system under the excitation caused by low frequency sway motions of the host structure. The case study presented in the paper demonstrates the effectivness of the proposed modelling approach to predict the dynamic behaviour of the system.

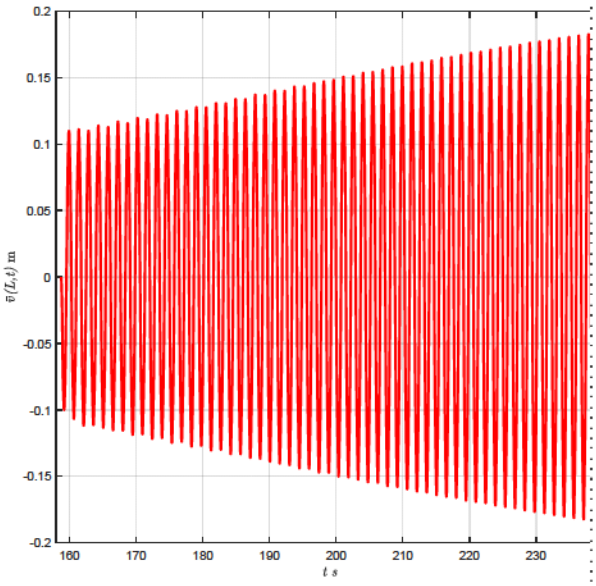

Figure 4. The lateral displacements $\overline{v}_M = \overline{v}(L,t)$ of the mass.

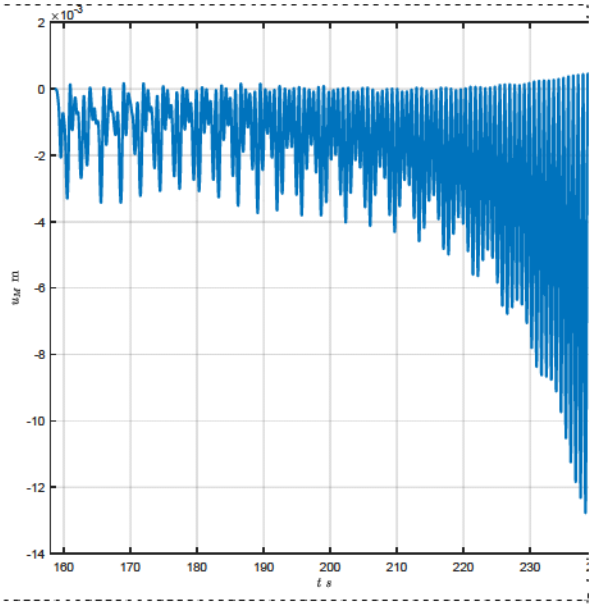

Figure 5. The longitudinal displacements $u_M(t)$ of the mass.

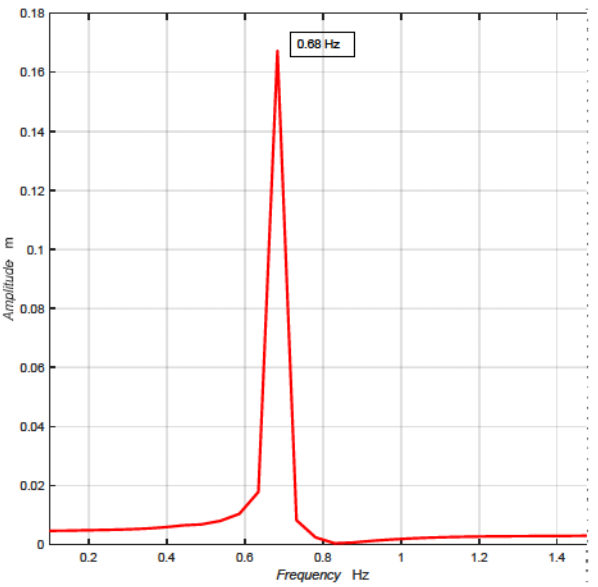

Figure 6. The frequency spectrum of the lateral response $\overline{v}_M = \overline{v}(L,t)$ of the mass.

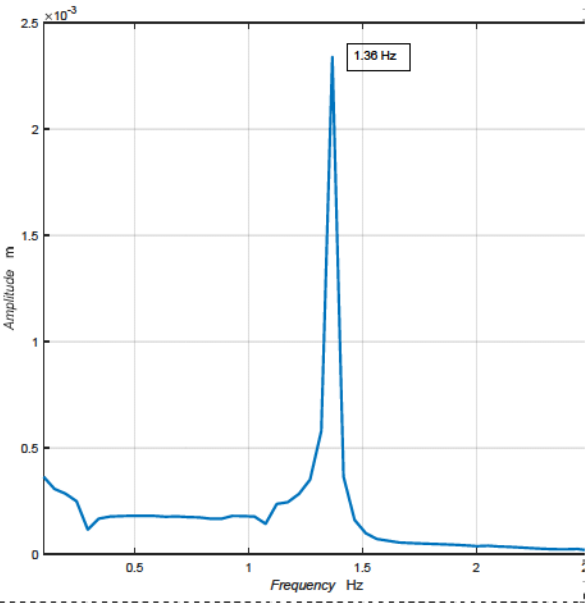

Figure 7. The frequency spectrum of the longitudinal response $u_M(t)$ of the mass.

References

[1] Hu R P, Xu Y L and Zhao X 2017 Long-Period Ground Motion Simulation and its Impact on Seismic Response of High-Rise Buildings *Journal of Earthquake Engineering* doi: 10.1080/13632469.2017.1286617

[2] Yao G C 2001 Performance of Passenger Elevators in Taiwan *Earthquake Engineering and Engineering Seismology* **3**(2) pp 17-26

[3] Saito T 2016 Response of High-Rise Buildings under Long Period Earthquake Ground Motions *International Journal of Structural and Civil Engineering Research* **5**(4) pp 308-314

[4] Meirovitch L 1990 *Dynamics and Control of Structures* (New York: John Wiley)

[5] Nayfeh A H and Pai P F 2004 *Linear and Nonlinear Structural Mechanics* (New York: John Wiley)

[6] Kaczmarczyk S and Iwankiewicz R 2017 Gaussian and non-Gaussian stochastic response of slender continua with time-varying length deployed in tall structures *International Journal of Mechanical Sciences* **134** pp 500-510

[7] Park S and Chung J 2014 Dynamic analysis of an axially moving finite-length beam with intermediate spring supports *Journal of Sound and Vibration* **333** pp 6742–6759